Simulating short-range order in compositionally complex materials

Ferrari, Alberto; Körmann, Fritz; Asta, Mark; Neugebauer, Jörg

DOI
10.1038/s43588-023-00407-4

Publication date
2023

Document Version
Final published version

Published in
Nature Computational Science

nature computational science

Review Article

https://doi.org/10.1038/s43588-023-00407-4

Simulating short-range order in compositionally complex materials

Received: 25 August 2022

Accepted: 30 January 2023

Published online: 31 March 2023

Check for updates

Alberto Ferrari[1], Fritz Körmann[1,2] ✉, Mark Asta[3,4] & Jörg Neugebauer[2] ✉

In multicomponent materials, short-range order (SRO) is the development of correlated arrangements of atoms at the nanometer scale. Its impact in compositionally complex materials has stimulated an intense debate within the materials science community. Understanding SRO is critical to control the properties of technologically relevant materials, from metallic alloys to functional ceramics. In contrast to long-range order, quantitative characterization of the nature and spatial extent of SRO evades most of the experimentally available techniques. Simulations at the atomistic scale have full access to SRO but face the challenge of accurately sampling high-dimensional configuration spaces to identify the thermodynamic and kinetic conditions at which SRO is formed and what impact it has on material properties. Here we highlight recent progress in computational approaches, such as machine learning-based interatomic potentials, for quantifying and understanding SRO in compositionally complex materials. We briefly recap the key theoretical concepts and methods.

Compositionally complex materials (CCMs)[1–4], including medium- and high-entropy alloys and ceramics, are crystalline mixtures of many elements in concentrated compositions. Unlike standard materials, where the alloying elements are diluted in one or two elements, CCMs have three or more principal components. This enables the exploration of larger portions of high-dimensional multicomponent phase diagrams, leading to superior design flexibility and tunability, which can be exploited to improve mechanical[5–11], physical (transport, electronic and magnetic)[12–19] and chemical[20–23] properties.

Compositional complexity often translates into a more complicated atomistic structure, because, in contrast to pure elements, mixtures generally break the crystal symmetry because of configurational arrangements of the chemical species over the sites of the underlying parent lattice, coupled with local distortions of the atoms away from them. Many recent investigations of CCMs have focused on determining a realistic atom-by-atom picture for these materials and on characterizing the degree of order or disorder at the atomistic level. This is of utmost importance for the understanding and design of materials, as the details of the atomistic structure often have direct consequences for the performance of a material. In this Review we first discuss how the local configurations of atoms are characterized, if and how they deviate from randomness by forming local order, and if and how they impact the microscopic and macroscopic properties of CCMs. To do this, we revisit how ordering can emerge in CCMs and how to distinguish long- and short-range ordering.

In thermodynamic equilibrium, the atomistic structure of CCMs is determined by the balance of three factors: (1) internal energy, related to the strength of the interatomic bonds, (2) vibrational entropy, which favors the formation of bonds with softer force constants, and (3) configurational entropy, which tends to favor configurations with a large number of possible realizations. External thermodynamic parameters, among which the prime example is temperature, tip this balance in favor of order or disorder. If the atomistic structure is periodically repeated in space, a material is said to possess long-range order (LRO). For CCMs, LRO is common only at low temperature. At high temperature, materials tend to lose LRO, which goes along with a phase transition, but correlations between atoms may still persist over finite spatial ranges (for example, several neighbor shells), and the atomistic configuration may not be completely random because the strength between certain pairs (or triplets, quadruplets and so on) of elements

[1]Materials Science and Engineering, Delft University of Technology, Delft, The Netherlands. [2]Max-Planck-Institut für Eisenforschung GmbH, Düsseldorf, Germany. [3]Materials Science and Engineering, University of California, Berkeley, CA, USA. [4]Materials Sciences Division, Lawrence Berkeley National Laboratory, Berkeley, CA, USA. ✉e-mail: koermann@mpie.de; neugebauer@mpie.de

https://doi.org/10.1038/s43588-023-00407-4

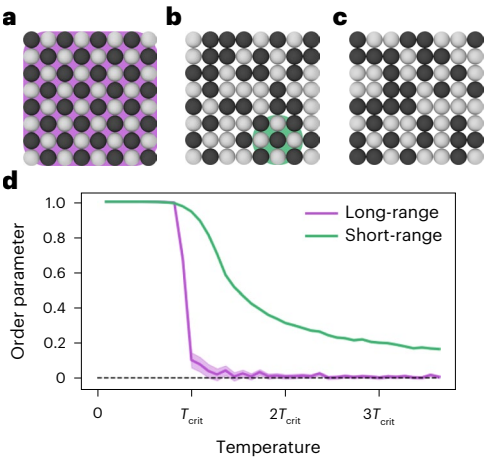

Fig. 1 | Long- and short-range order. a–**c**, Low- (**a**), medium- (**b**) and high- (**c**) temperature configurations of a two-dimensional binary alloy with attractive interactions between opposite-type pairs. Purple and green shaded areas indicate LRO and SRO, respectively. **d**, Temperature dependence of the LRO and SRO parameters. The shaded area indicates typical statistical error bars.

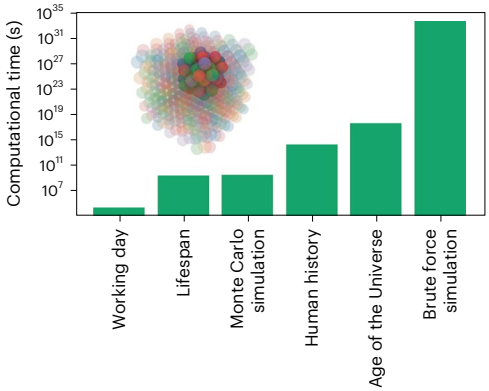

Fig. 2 | Gigantic chemical phase space requires a large amount of computational resources. The estimated time required to sample all the possible configurations in the first three neighbor shells (see inset) of a quinary alloy (`brute force') or to perform a million Monte Carlo steps with DFT, compared to the length of a working day, the average human lifetime, the whole span of human history and the age of the Universe. For the DFT calculations, we assumed a typical time of 1 h for each configuration.

might be stronger than others. In this case, a material is said to possess short-range order (SRO). SRO is particularly relevant for CCMs given the increased variability of the chemical species.

The difference between LRO and SRO is best exemplified by considering a model system with two atomic species (Fig. 1, black and white) that occupy a square lattice. For simplicity, we can assume that the atoms interact only with their nearest neighbors and that there is a net attraction between opposite species. As shown in Fig. 1, a long-range-ordered chessboard pattern arises at low temperature because opposite-type pairs tend to form nearest-neighbor bonds. This LRO disappears at T_{crit} (Fig. 1d, magenta line, corresponding to the LRO parameter, defined as the difference in composition of black atoms on the two sublattice sites of the checkerboard structure). Above T_{crit}, opposite-type pairs are not able to arrange in a regular pattern, but they still tend to attract each other more than same-type pairs. This imbalance leads to SRO.

The easiest way to quantify SRO is to use the Warren–Cowley parameters[24,25], which measure to what extent the correlation between pairs of elements i and j deviate from randomness. The Warren–Cowley parameters for multicomponent materials are defined as

$$\alpha_{ij}^{m} = 1 - \frac{p_{ij}^{m}}{c_i c_j}, \quad (1)$$

where p_{ij}^{m} is the probability of finding i–j neighbors in the mth shell, and c_i and c_j are the concentrations of i and j, respectively. We note that p_{ij}^{m} is equal to the product $c_i c_j$ if sites i and j are uncorrelated, as they would be in a random alloy, where $\alpha_{ij}^{m} = 0$ for all shells m. By contrast, the Warren–Cowley parameters are negative (positive) if elements i and j tend to attract (repel) each other. The green line in Fig. 1 shows α_{00}^{1}, that is, the black–black (or equivalently white–white) correlation at the first neighbor shell. It can be clearly seen that same-type pairs repel each other up to very high temperature, indicating that SRO may be active even up to the melting point of a material[26].

Qualitative analysis of the simple model in Fig. 1 can be generalized to any non-ideal solid solution, meaning that, if the interactions among the components are not negligible, every mixture of elements possesses SRO. This naturally includes CCMs, for which, in most cases, the simultaneous presence of many elements enhances the imbalance among the atomic interactions and hence promotes SRO.

Although there is now consensus in the CCMs community that SRO is probably omnipresent, there is still debate about whether and how it can impact measurable materials properties[27,28]. The main reason behind this uncertainty is that, experimentally, it is very challenging to quantitatively measure the degree of SRO for all pairs (because it has a typical length scale of only a few nanometers) and to control SRO, as it is very sensitive to the processing conditions[29–32]. Moreover, SRO does not seem to be correlated with simple chemical descriptors (for example, atomic size mismatch or electronegativity difference)[33], but is instead driven by the strength of the interactions between pairs of elements[33,34]. Given the inherent difficulties of performing experiments, theoretical simulations have thus been critical in exploring this phenomenon.

One of the most popular methods to gain atomistic insights into CCMs is density functional theory (DFT). DFT is based on quantum mechanics and allows calculation of the total energy and forces of a system of atoms up to milli-electronvolt accuracy. Unfortunately, obtaining useful information on SRO directly from DFT is not straightforward. As displayed in Fig. 2, to sample all the possible configurations of just the first three neighbor shells around an atom in a quinary alloy with DFT (‘brute force’ simulation) would already take several orders of magnitude more time than the age of the Universe. This is because (1) the number of possible configurations is extremely large (5^{43} for a quinary alloy with a face-centered cubic lattice) and (2) the high accuracy of DFT comes at a high computational cost, deriving mainly from the repeated diagonalization of very large matrices.

The first problem can be addressed by ranking the configurations in terms of frequency/likelihood and sample only the most likely ones. According to Boltzmann’s statistics, high-energy configurations are exponentially less likely than low-energy configurations. The more likely configurations can be explored with the Metropolis Monte Carlo algorithm[35], which is several orders of magnitude more efficient than ‘brute force’ sampling, as shown in Fig. 2. However, Monte Carlo simulations still require substantial computational time if combined with DFT calculations, and existing works that rely only on DFT are often limited in terms of system size or number of configurations and also often rely on the assumption that atoms reside on ideal lattice sites[36–39]. To further decrease the computational time, the interatomic interactions must be parameterized with simpler models, and how to parameterize these interactions accurately and efficiently is actually one of the main challenges currently faced by the computational materials science community.

https://doi.org/10.1038/s43588-023-00407-4

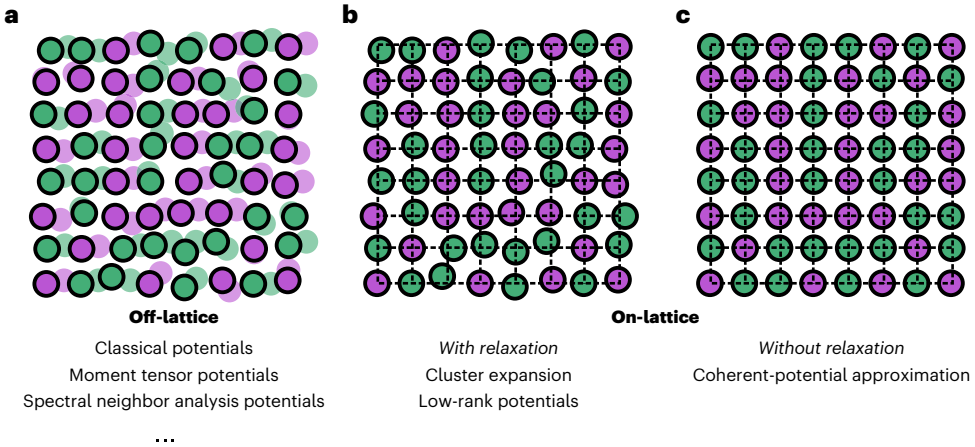

Fig. 3 | Off-lattice and on-lattice models. a, Off-lattice models, capturing chemical configurations and the full atomic degrees of freedom. **b**, On-lattice models, allowing the inclusion of atomic distortion energies. **c**, On-lattice models, restricted to the ideal lattice positions.

In this Review we discuss how SRO is currently investigated with computer simulations and how, based on these simulations, it is predicted to change the properties of CCMs.

Interatomic interactions in many dimensions

The problem inherent to sampling millions of configurations with DFT is its low computational efficiency. To address this issue, energies and forces derived from quantum mechanics must be obtained from a simpler mathematical format for the interatomic interactions between atoms, but finding accurate interactions that best mimic the multi-body relations between real atoms is not straightforward. This problem is even more difficult for CCMs, because these interactions usually depend strongly on the chemical environment, which is characterized by a high variance when many elements are mixed together. Mathematically, this means that the domain of the functions that describe the interactions is high-dimensional, so exponentially larger databases are required for the fitting (the curse of dimensionality).

Especially when they are used to characterize ordering mechanisms, the methods to obtain interatomic interactions are distinguished as off-lattice and on-lattice models (Fig. 3). In off-lattice models, the energy of an atom i is a direct function of the positions $\mathbf{R}$ and chemical species Z of its N neighbors, and hence the total energy of a particular configuration $\boldsymbol{\sigma}$ is given by

$$E_{\text{off-latt}}(\boldsymbol{\sigma}) = \sum_i E_i(\boldsymbol{\sigma}_i),\ \boldsymbol{\sigma}_i = (\mathbf{R}_1, ..., \mathbf{R}_N; Z_1, ..., Z_N). \quad (2)$$

In on-lattice models, the atomic displacements with respect to the ideal lattice sites are assumed to be small, allowing for an affine mapping of the equilibrium atomic positions to the underlying crystal lattice sites. In practice, this requirement limits applications to systems that are dynamically stable, that is, to those for which atomic distortions do not alter the atomic environments substantially. The energy of an atom i thus depends only on the decoration of chemical species around it:

$$\begin{aligned} E_{\text{on-latt}}(\tilde{\boldsymbol{\sigma}}) &= \min_{\mathbf{R}} E_{\text{off-latt}} \\ &= \sum_i \tilde{E}_i(\tilde{\boldsymbol{\sigma}}_i),\ \tilde{\boldsymbol{\sigma}}_i = (Z_1, ..., Z_N). \end{aligned} \quad (3)$$

Atomic coordinates are not entered explicitly in this model and therefore the computational complexity is dramatically reduced.

The traditional approaches used to parameterize interatomic interactions are (1) cluster expansion[40], an on-lattice model that considers the total energy of a system as a sum of contributions from multi-body figures of atoms (pairs, triplets, quadruplets and so on) up to a given distance threshold, and (2) classical potentials[41,42], off-lattice models that assume a physically motivated functional form for the interactions and fit the parameters of this form to reproduce a set of properties. These approaches provide reasonable accuracy for binary or ternary systems. However, they become increasingly intractable for materials containing larger numbers of components, such as CCMs, and are potentially less accurate due to the challenge of adequately sampling the configuration space in their training for such systems. This challenge is mainly related to the fact that the number of fitting parameters is inadequate: too large for cluster expansion, yielding impractical fitting, and too small for classical potentials, yielding poor accuracy. Moreover, neither of these methods, at least as proposed originally, can treat magnetism, which is intimately connected with SRO for some materials[43].

Another class of approaches, more efficient for CCMs, exploits the coherent-potential approximation[44,45], a mean-field treatment that introduces an effective medium to model the varying potential of different atoms in an alloy. With these approaches it is possible to calculate the interactions between pairs of atoms in real space (with the generalized perturbation method[46], based, for example, on the exact muffin-tin orbital formalism[47]) or in reciprocal space (with concentration wave analysis[48], based, for example, on the Korringa–Kohn–Rostoker Green's function method[49]) and hence to derive approximate SRO and LRO tendencies. The main drawback of these mean-field approximations is that they cannot incorporate atomic distortions, which have been observed to qualitatively impact ordering mechanisms[50]. This is due to the fact that atomic displacements can give rise to sizable strain-mediated interactions that can qualitatively and quantitatively change the nature of the SRO[51,52].

The limitations of such conventional approaches have led to the development and application of a new generation of methods based on the concepts of machine learning. These approaches can be viewed as improvements and generalizations of the traditional cluster expansion and classical potentials methods, with the application of data science techniques, such as regularization or feature engineering. Although many formalisms to derive the interatomic interactions have been proposed, only a few have proven accurate enough to treat CCMs.

The conventional cluster expansion can be made more robust for CCMs by applying feature selection and dimensionality reduction to decrease the number of parameters before fitting. It has been shown that preselecting the most important interactions with the Bayesian information criterion[53], or applying principal component analysis[54], substantially improves the quality of cluster expansion for CCMs.

https://doi.org/10.1038/s43588-023-00407-4

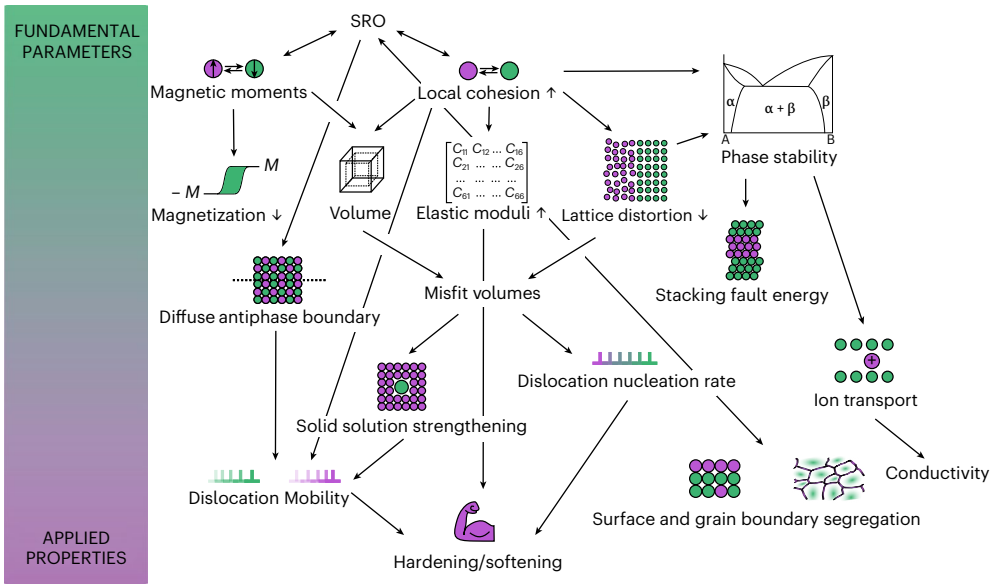

Fig. 4 | Consequences of SRO. A concept map showing the features and consequences of SRO in relation to the fundamental parameters (top) and applied properties of CCMs (bottom). The schematic shows how SRO can directly impact fundamental properties (the intrinsic coupling of local magnetic moments and local cohesion is indicated by double arrows) and indirectly a number of applied materials properties (for example, mechanical properties or conductivity).

Furthermore, addition of a penalty term to regularize more complex models during fitting (for example, by adding the norm of the fitting parameters to the cost function) also improves the regression of the interaction parameters[54,55].

Classical potentials can instead be enhanced by increasing the number of parameters, up to the point of no longer even requiring the definition of a specific function. This leads to the development of machine learning potentials, which are currently the state-of-the-art method for modeling interatomic interactions with near-DFT accuracy.

One of the most popular classes of machine learning potentials used to study SRO in CCMs is that of low-rank potentials (LRPs)[56], a class of systematically improvable on-lattice potentials suited for Monte Carlo simulations. Like cluster expansion, LRPs establish a mapping between the local atomic arrangements of atoms and the energy, but are much more efficient when the training sets are sparse; that is, the parameter space is high-dimensional and the training databases are comparatively small. LRPs are based on tensor decomposition techniques, generalizations of the matrix factorization algorithms used, for example, by product recommendation systems in electronic commerce[57].

Like all on-lattice models, the main disadvantage of LRPs is that they cannot explicitly include atomic vibrations, which may contribute to SRO at finite temperature. Off-lattice machine learning potentials, among which moment tensor potentials (MTPs)[58] and spectral neighbor analysis potentials (SNAPs)[59], lift this approximation of a static lattice by parameterizing the interatomic interactions as a function of the distance and angles between a central atom and the atoms in its neighborhood. The different flavors of machine learning potentials proposed in recent years differ from each other in the features they use to represent the neighborhood of an atom, and compete to provide an as-complete representation as possible at the least computational cost. Machine learning potentials are therefore promising for tackling computational problems that are, on the one hand, too expensive to be solved by DFT directly (for example, problems requiring very large supercells or long simulation times), but for which, on the other hand, a computational accuracy is required that cannot be achieved by classical potentials. Some examples are given in the following.

Three examples in the literature show that traditional methods may be inadequate for CCMs and that machine learning potentials could be more appropriate. (1) For the MoNbTaW alloy, approaches based on the coherent-potential approximation and cluster expansion[60–62] indicated that this system partitions into two ordered phases, one containing Mo and Ta and one containing W and Nb, but more recent calculations with an LRP showed that this is an artifact of neglecting the atomic distortions and that another phase may be more stable[50]. (2) For the MoNbTaVW alloy, it was shown that MTPs are much more accurate than classical potentials to calculate the vibrational contributions to the free energy up to the melting point[63]. (3) A classical potential fitted for the CrCoNi alloy[64] and used in many investigations exhibits qualitatively different Warren–Cowley parameters with respect to recent machine learning potentials[65] and DFT[37,39]. The classical potential also predicts a tendency for the alloy to decompose into Ni-rich and CrCo-rich domains, which has so far not been observed in DFT nor in experiments.

SRO and its impact on materials properties

The advancement of the computational techniques used to characterize SRO in recent years, especially with the advent of machine learning potentials, has led to a better understanding of this phenomenon. As most of these techniques have been developed only very recently, the majority of SRO investigations discussed in the following were performed based on explicit DFT calculations. SRO has been observed in many CCMs, including (1) the famous Cantor alloy, CrMnFeCoNi, and some of its subsystems[37,66,67], also with the addition of Al[68,69], Cu[70] or Pd[71]; (2) alloys of the refractory elements Ti, V, Cr, Zr, Nb, Mo, Hf, Ta and W[60,61,72–75]; (3) more diverse combinations of elements, such as VCoNi[76], Co–Fe–Ni–Ti[74,77], Al–Cr–Fe–Ni–Ti[78], AlNbTiV[79], AlHfNbTaTiZr and their subsystems[54]; and (4) multication ceramics with rocksalt[80] and pyrochlore[81] structures. Despite the abundance of observations, however, details of how this mechanism impacts CCMs are still not fully clear.

In this section, we discuss the implications of SRO regarding fundamental materials parameters, related to basic thermodynamical, mechanical or chemical features, and applied properties, involving more complex mechanisms (mechanical response, ionic transport, for example) or structures (defects). The impact of SRO on fundamental

parameters is generally well understood from the atomistic point of view, but lacks experimental validation. On the other hand, the impact of SRO on some applied properties is still under debate from both theoretical and experimental points of view.

To give an impression of how fundamental parameters and applied properties are intertwined with each other and how both may be influenced by SRO, we sketch in Fig. 4 the key concepts that will be discussed in this section. The advantage of investigating SRO and its consequences with computer simulations, in contrast to experiments, is that individual features can be independently resolved for the purpose of clarifying how different mechanisms ultimately impact the performance of a material.

SRO and fundamental materials parameters

Atomistic simulations clearly indicate that SRO can have direct impact on the physical properties of CCMs. For example, when the degree of SRO increases, the elastic moduli generally increase because the internal energy decreases[38,67,77,82,83], and in magnetic alloys the magnetization can decrease because antiferromagnetic configurations may be formed[38,68]. Changes in cohesion and magnetic properties could in turn also impact the equilibrium volume[43].

Phase stability. Besides the physical properties, the most obvious aspect that is affected by ordering is phase stability. This can be studied with the on-lattice interatomic machine learning potentials discussed in the previous section. SRO always decreases both the enthalpy and the configurational entropy of a phase[84], and the competition between these two contributions determines the degree of SRO as a function of temperature. Calculation of phase diagrams (CALPHAD) simulations[34] has estimated that the excess Gibbs energy due to SRO can be of the order of −10 meV per atom. SRO can also have an influence on order–disorder transition temperatures, as observed in CrCoNi for the phase transformation responsible for the so-called 'K-state' phenomenon, that is the abnormal change of physical properties as a function of temperature[85]. The term 'K-state' originates from the German 'Komplexer Zustand' ('complex state'). Moreover, SRO often signals incipient ordering tendencies that may manifest at low temperature, for example, the precipitation of ordered phases in MoNbTaW[60], AlNbTiV[79], VCoNi[76], Al–Cr–Fe–Ni–Ti[78,86] and Cr–Ta–Ti–V–W[73].

We note that the majority of recent simulations for SRO assume on-lattice approaches and typically do not account for thermal excitations, which could, as discussed above, also impact phase stability. To study such effects, accurate but computationally and conceptually much more demanding off-lattice potentials are required to perform coupled Monte Carlo and molecular dynamics simulations, for example.

Stacking fault energy. In face-centered cubic and hexagonal close-packed CCMs, SRO can impact the stacking fault energy, that is, the energy required to create a planar defect in the periodic stacking of atomic layers. DFT calculations, in combination with Monte Carlo techniques, showed that the stacking fault energy depends strongly on the composition near the fault[87–89]. This can result in local arrangements rendering the stacking fault energies positive and, for some other arrangements, negative.

The change in stacking fault energy can also be related to phase stability. In face-centered cubic alloys, the stacking fault energy generally increases with increasing SRO, as shown by combined Monte Carlo and ab initio calculations[39,64]. This means that, for alloys for which the face-centered cubic arrangement is thermodynamically stable, SRO decreases the energy of the face-centered cubic structure more as compared to hexagonal close-packed structures. Higher stacking fault energies result in smaller equilibrium separation distances between partial dislocations, as observed in simulations employing carefully constructed classical potentials and molecular dynamics simulations[64] and experiments[32].

Magnetism. In magnetic materials, the relief of magnetically frustrated configurations may be a driving force towards the formation of SRO. Clear examples are the ordering of Cr in CrCoNi and CrFeCoNi[37,43,66,90,91] and of Mn in MnFeCoNi[68]: Cr and Mn generally prefer an antiferromagnetic configuration and hence tend to avoid binding with other Cr or Mn atoms in the first neighbor shell, so that their magnetic moment is antiparallel to that of Fe, Co and Ni.

In certain CCMs, such as CrCoNi, because of stoichiometric constraints, antiferromagnetic elements cannot have only ferromagnetic elements as first neighbors. The existing nearest-neighbor pairs of the elements that would prefer the antiferromagnetic configuration usually tend to have opposite spins, and this results in a magnetic SRO[43] that adds on top of the chemical SRO.

It is worth mentioning that most studies coupling magnetism and SRO have so far been performed using explicit DFT calculations either in conjunction with Monte Carlo simulations or based on the coherent-potential approximation to mimic chemical disorder. Although local lattice distortions are not explicitly accounted for in the latter approach, magnetic effects can be more straightforwardly modeled (for example, using the disordered-local-moment method). This exemplifies once more the need for a next generation of machine learning potentials including magnetism to better understand the inherent interplay of distortions, vibrations and magnetism in CCMs.

Lattice distortion and misfit volumes. Because it homogenizes the lattice, SRO usually decreases the average lattice distortion in CCMs[76]. The reduction of lattice distortion usually results in a decreased availability of nucleation sites for new phases or defects, and this, in turn, may increase the melting temperature[92] or affect solid–solid phase transitions, for example.

The change in lattice distortion may also have consequences for misfit volumes, that is, variations in the volume per atom for small changes in composition, which are very important input parameters for solid solution strengthening theories of CCMs[93,94]. Changes in misfit volumes determine variations in the elastic contribution to hardening[74,77], but also in the dislocation nucleation rate[95,96], and thus ultimately impact mechanical properties. These contributions tend to compete with each other, and whether higher or lower misfit volumes result in softening or in hardening differs from material to material.

Yin and colleagues[27] observed experimentally that misfit volumes of the component elements in CrCoNi are similar to those measured in the binaries Cr–Co, Co–Ni and Cr–Ni, and they thus concluded that the role of SRO is negligible. They also claimed that misfit volumes are poorly predicted by DFT for this material. On the other hand, Walsh and colleagues[43] showed, for the same material, that the experimentally measured misfit volumes can be obtained from DFT if a model for the composition-dependent chemical and magnetic SRO is taken into account. These apparently contradicting conclusions show that the impact of SRO on the misfit volumes of CrCoNi is still a matter of debate. A negligible effect of SRO on misfit volumes was predicted for NbHfTiZr[83] based on DFT.

Impact of SRO on applied materials properties

The impact of SRO on the fundamental materials parameters of CCMs has an effect on their applied properties too. For example, the change in misfit volumes influences the mechanical properties, and the change in the phase stability influences the composition of defects and ion transport in ceramics. To understand to what degree SRO can lead to modifications of applied materials properties will be pivotal for CCM design, as SRO could be engineered to optimize desired features or hamper detrimental mechanisms.

Dislocation mobility. SRO can have opposite effects on the dislocation mobility. In general, SRO promotes the formation of diffuse antiphase

boundaries[77,97] and increases local cohesion[64], both of which decrease the mobility of dislocations. However, SRO also homogenizes the lattice, which may result in a decrease in the solid solution strengthening and hence in an increase of dislocation mobility[74]. As already mentioned, the competition of these mechanisms can lead either to hardening or softening of CCMs. To resolve this, highly accurate and efficient potentials are required, providing an excellent opportunity for the machine learning potentials introduced above (Interatomic interactions in many dimensions section). With an MTP, the aforementioned duality was eventually observed in MoNbTaW simulations[98]. In this material, SRO slows down screw dislocations, because of the formation of diffuse antiphase boundaries that decrease the nucleation rate of kink pairs, but at the same time it speeds up edge dislocations, due to lower solute drag. Note that in body-centered cubic alloys such as MoNbTaW, screw dislocations determine plasticity at low temperature, whereas edge dislocations do so at high temperature[94,98]. Accordingly, the overall impact of SRO on mechanical properties might strongly depend on temperature for this CCM.

For CrCoNi, simulations with a classical potential indicated that SRO decreases the energy of local configurations, thereby increasing the Peierls barrier to unpin dislocations[64], and decreases the dislocation nucleation rate[95,96]. The combination of these factors should result in a substantial hardening of CrCoNi. However, this is not backed up by experiments[27,32]. The hardness and yield strength of this CCM do not change with different annealing conditions, suggesting that SRO has a negligible impact on the bulk mechanical properties of CrCoNi. We note, however, that differences in nanoindentation responses are observed with different annealing conditions, suggesting the effects of SRO[32]. Similar conclusions for the bulk were also drawn from simulations for the quinary CrMnFeCoNi alloy[28]. As already mentioned, the confusion may derive from the use of an inaccurate classical potential, which predicts an incorrect partitioning of Ni/CrCo at low temperature. To resolve these limitations, more accurate machine learning potentials, possibly considering magnetism, would be required.

Segregation at extended defects. SRO is intimately connected with the segregation at extended defects, such as surfaces, grain boundaries and faults. SRO can change the chemical potential of the component elements in the bulk, while segregation mechanisms can in turn alter the Warren–Cowley parameters[99]. Furthermore, segregation may induce another type of SRO, consisting of local rearrangements of the atoms in the vicinity of the defects: the atomic layers adjacent to a defect are usually enriched in the elements that preferentially bind to the segregating elements and this ordering can extend for a couple of layers in the bulk.

SRO on the surfaces of CCMs appears to be stronger than in the bulk, and it seems that the more open the surface, the larger the magnitude of the Warren–Cowley parameters[100]. This trend may be related to the fact that fewer bonds are available on more open structures, and so ordering is enhanced. Monte Carlo simulations are typically used to capture ordering effects near extended defects. The quality of these simulations is decided by the accuracy of the parameterization of the interatomic interactions, and classical potentials may sometimes not be appropriate. For example, a classical potential for CrMnFeCoNi suggested an incorrect segregation of Mn[101,102], whereas DFT calculations indicate that Ni is the segregating element, at least under vacuum conditions[103]. This again highlights the need for accurate machine learning potentials to study segregation in CCMs.

Future directions and opportunities

Despite the substantial effort to investigate SRO in CCMs in the last few years, characterization of this phenomenon is still in its infancy, and a deeper understanding of the connection between the atomistic structure and fundamental and applied properties is required before SRO can be exploited for materials design.

From a technical point of view, machine learning potentials still have large room for improvement. For example, introducing a scheme to automatically detect extrapolation and add structures to the training database if the extrapolation is too severe (active learning)[104] could address the issues related to sparseness of the fitting data and the transferability of potentials. Furthermore, explicit inclusion of magnetism in the potentials formalism may further increase accuracy for magnetic materials, such as the Cantor alloy and its subsystems[105]. Off-lattice models could also address the interplay of SRO and thermal excitations (for example, vibrations), which at the present time is unknown.

In comparison to classical potentials, machine learning potentials suffer from two important drawbacks. First, given the large number of fitting parameters, they require large training databases, which need to be compiled with DFT and hence can be computationally expensive to generate. Second, machine learning potentials are characterized by poor transferability to structures and compositions not included in the training set. However, for most CCMs, it seems that machine learning potentials are very promising to effectively describe complex interatomic interactions.

An all-round characterization of SRO in CCMs would benefit from new theoretical techniques and computational algorithms to address the impact of SRO on kinetic parameters, such as diffusion barriers, and the energetics of point defects, such as vacancies and interstitials. Furthermore, a grand challenge for future generations of simulations and experiments is the investigation of SRO outside thermodynamic equilibrium; that is, what are the relevant timescales for the formation and dissolution of ordering. These aspects are important to bring simulations and experiments closer together, as SRO is usually studied in quenched samples that may be frozen into a non-equilibrium state.

References

1. Yeh, J.-W. et al. Nanostructured high-entropy alloys with multiple principal elements: novel alloy design concepts and outcomes. *Adv. Eng. Mater.* **6**, 299–303 (2004).
2. Cantor, B., Chang, I. T. H., Knight, P. & Vincent, A. J. B. Microstructural development in equiatomic multicomponent alloys. *Mater. Sci. Eng. A* **375–377**, 213–218 (2004).
3. George, E. P., Raabe, D. & Ritchie, R. O. High-entropy alloys. *Nat. Rev. Mater.* **4**, 515–534 (2019).
4. Oses, C., Toher, C. & Curtarolo, S. High-entropy ceramics. *Nat. Rev. Mater.* **5**, 295–309 (2020).
5. Senkov, O. N., Wilks, G. B., Scott, J. M. & Miracle, D. B. Mechanical properties of $Nb_{25}Mo_{25}Ta_{25}W_{25}$ and $V_{20}Nb_{20}Mo_{20}Ta_{20}W_{20}$ refractory high entropy alloys. *Intermetallics* **19**, 698–706 (2011).
6. Gali, A. & George, E. P. Tensile properties of high- and medium-entropy alloys. *Intermetallics* **39**, 74–78 (2013).
7. Otto, F. et al. The influences of temperature and microstructure on the tensile properties of a CoCrFeMnNi high-entropy alloy. *Acta Mater.* **61**, 5743–5755 (2013).
8. Gludovatz, B. et al. A fracture-resistant high-entropy alloy for cryogenic applications. *Science* **345**, 1153–1158 (2014).
9. Gludovatz, B., George, E. P. & Ritchie, R. O. Processing, microstructure and mechanical properties of the CrMnFeCoNi high-entropy alloy. *JOM* **67**, 2262–2270 (2015).
10. Sarker, P. et al. High-entropy high-hardness metal carbides discovered by entropy descriptors. *Nat. Commun.* **9**, 4980 (2018).
11. Ferrari, A., Lysogorskiy, Y. & Drautz, R. Design of refractory compositionally complex alloys with optimal mechanical properties. *Phys. Rev. Mater.* **5**, 063606 (2021).
12. Bérardan, D., Franger, S., Dragoe, D., Meena, A. K. & Dragoe, N. Colossal dielectric constant in high entropy oxides. *Phys. Status Solidi RRL* **10**, 328–333 (2016).
13. Bérardan, D., Franger, S., Meena, A. & Dragoe, N. Room temperature lithium superionic conductivity in high entropy oxides. *J. Mater. Chem. A* **4**, 9536–9541 (2016).

14. Meisenheimer, P., Kratofil, T. & Heron, J. Giant enhancement of exchange coupling in entropy-stabilized oxide heterostructures. *Sci. Rep.* **7**, 13344 (2017).
15. Braun, J. L. et al. Charge-induced disorder controls the thermal conductivity of entropy-stabilized oxides. *Adv. Mater.* **30**, 1805004 (2018).
16. Ma, Y. et al. High-entropy metal-organic frameworks for highly reversible sodium storage. *Adv. Mater.* **33**, 2101342 (2021).
17. Wagner, C. et al. Effects of Cr/Ni ratio on physical properties of Cr-Mn-Fe-Co-Ni high-entropy alloys. *Acta Mater.* **227**, 117693 (2022).
18. Zhang, Y., Osetsky, Y. N. & Weber, W. J. Tunable chemical disorder in concentrated alloys: defect physics and radiation performance. *Chem. Rev.* **122**, 789–829 (2021).
19. Li, Y. et al. Chemical ordering effect on the radiation resistance of a CoNiCrFeMn high-entropy alloy. *Comput. Mater. Sci.* **214**, 111764 (2022).
20. Yao, Y. et al. Carbothermal shock synthesis of high-entropy-alloy nanoparticles. *Science* **359**, 1489–1494 (2018).
21. Löffler, T. et al. Discovery of a multinary noble metal-free oxygen reduction catalyst. *Adv. Energy Mater.* **8**, 1802269 (2018).
22. Xie, P. et al. Highly efficient decomposition of ammonia using high-entropy alloy catalysts. *Nat. Commun.* **10**, 4011 (2019).
23. Zhang, N. et al. Lattice oxygen activation enabled by high-valence metal sites for enhanced water oxidation. *Nat. Commun.* **11**, 4066 (2020).
24. Cowley, J. An approximate theory of order in alloys. *Phys. Rev.* **77**, 669–675 (1950).
25. Norman, N. & Warren, B. E. X-ray measurement of short range order in Ag-Au. *J. Appl. Phys.* **22**, 483 (1951).
26. Wang, M., Guo, S., Lin, X. & Huang, W. Research on the nucleation and growth of high-entropy alloy. *Mater. Lett.* **285**, 129206 (2021).
27. Yin, B., Yoshida, S., Tsuji, N. & Curtin, W. A. Yield strength and misfit volumes of NiCoCr and implications for short-range-order. *Nat. Commun.* **11**, 2507 (2020).
28. Zhou, D. et al. Effects of annealing on hardness, yield strength and dislocation structure in single crystals of the equiatomic Cr-Mn-Fe-Co-Ni high entropy alloy. *Scripta Mater.* **191**, 173–178 (2021).
29. Zhang, F. X. et al. Local structure and short-range order in a NiCoCr solid solution alloy. *Phys. Rev. Lett.* **118**, 205501 (2017).
30. Ma, Y. et al. Chemical short-range orders and the induced structural transition in high-entropy alloys. *Scripta Mater.* **144**, 64–68 (2018).
31. Schönfeld, B. et al. Local order in Cr-Fe-Co-Ni: experiment and electronic structure calculations. *Phys. Rev. B* **99**, 014206 (2019).
32. Zhang, R. et al. Short-range order and its impact on the CrCoNi medium-entropy alloy. *Nature* **581**, 283–287 (2020).
33. Chen, S. et al. Chemical-affinity disparity and exclusivity drive atomic segregation, short-range ordering, and cluster formation in high-entropy alloys. *Acta Mater.* **206**, 116638 (2021).
34. Abe, T. Effect of short-range ordering in high-entropy alloys. *Mater. Trans.* **62**, 711–718 (2021).
35. Metropolis, N., Rosenbluth, A. W., Rosenbluth, M. N., Teller, A. H. & Teller, E. Equation of state calculations by fast computing machines. *J. Chem. Phys.* **21**, 1087–1092 (1953).
36. Widom, M., Huhn, W. P., Maiti, S. & Steurer, W. Hybrid Monte Carlo/molecular dynamics simulation of a refractory metal high entropy alloy. *Metall. Mater. Trans. A* **45**, 196–200 (2014).
37. Tamm, A., Aabloo, A., Klintenberg, M., Stocks, M. & Caro, A. Atomic-scale properties of Ni-based FCC ternary, and quaternary alloys. *Acta Mater.* **99**, 307–312 (2015).
38. Feng, W., Qi, Y. & Wang, S. Effects of short-range order on the magnetic and mechanical properties of FeCoNi(AlSi)$_x$ high entropy alloys. *Metals* **7**, 482 (2017).
39. Ding, J., Yu, Q., Asta, M. & Ritchie, R. O. Tunable stacking fault energies by tailoring local chemical order in CrCoNi medium-entropy alloys. *Proc. Natl Acad. Sci. USA* **115**, 8919–8924 (2018).
40. Sanchez, J. M., Ducastelle, F. & Gratias, D. Generalized cluster description of multicomponent systems. *Phys. A* **128**, 334–350 (1984).
41. Daw, M. S. & Baskes, M. I. Semiempirical, quantum mechanical calculation of hydrogen embrittlement in metals. *Phys. Rev. Lett.* **50**, 1285–1288 (1983).
42. Finnis, M. W. & Sinclair, J. E. A simple empirical *N*-body potential for transition metals. *Philos. Mag. A* **50**, 45–55 (1984).
43. Walsh, F., Asta, M. & Ritchie, R. O. Magnetically driven short-range order can explain anomalous measurements in CrCoNi. *Proc. Natl Acad. Sci. USA* https://doi.org/10.1073/pnas.2020540118 (2021).
44. Soven, P. Coherent-potential model of substitutional disordered alloys. *Phys. Rev.* **156**, 809–813 (1967).
45. Gyorffy, B. Coherent-potential approximation for a nonoverlapping-muffin-tin-potential model of random substitutional alloys. *Phys. Rev. B* **5**, 2382–2384 (1972).
46. Ducastelle, F. & Gautier, F. Generalized perturbation theory in disordered transitional alloys: applications to the calculation of ordering energies. *J. Phys. F* **6**, 2039 (1976).
47. Vitos, L. *Computational Quantum Mechanics for Materials Engineers: the EMTO Method and Applications* (Springer, 2007).
48. Singh, P., Smirnov, A. V. & Johnson, D. D. Atomic short-range order and incipient long-range order in high-entropy alloys. *Phys. Rev. B* **91**, 224204 (2015).
49. Faulkner, J., Stocks, G. M. & Wang, Y. *Multiple Scattering Theory; Electronic Structure of Solids* (Institute of Physics, 2018).
50. Kostiuchenko, T., Körmann, F., Neugebauer, J. & Shapeev, A. Impact of lattice relaxations on phase transitions in a high-entropy alloy studied by machine-learning potentials. *npj Comput. Mater.* **5**, 55 (2019).
51. Wolverton, C., Ozoliņš, V. & Zunger, A. First-principles theory of short-range order in size-mismatched metal alloys: Cu-Au, Cu-Ag and Ni-Au. *Phys. Rev. B* **57**, 4332–4348 (1998).
52. Reichert, H. et al. Competition between order and phase separation in Au-Ni. *Phys. Rev. Lett.* **95**, 235703 (2005).
53. Zhang, J. et al. Robust data-driven approach for predicting the configurational energy of high entropy alloys. *Mater. Design* **185**, 108247 (2020).
54. Nataraj, C., Borda, E. J. L., van de Walle, A. & Samanta, A. A systematic analysis of phase stability in refractory high entropy alloys utilizing linear and non-linear cluster expansion models. *Acta Mater.* **220**, 117269 (2021).
55. Géron, A. *Hands-On Machine Learning with Scikit-Learn, Keras, and TensorFlow: Concepts, Tools, and Techniques to Build Intelligent Systems* (O'Reilly Media, 2019).
56. Shapeev, A. Accurate representation of formation energies of crystalline alloys with many components. *Comput. Mater. Sci.* **139**, 26–30 (2017).
57. Koren, Y., Bell, R. & Volinsky, C. Matrix factorization techniques for recommender systems. *Computer* **42**, 30–37 (2009).
58. Shapeev, A. V. Moment tensor potentials: a class of systematically improvable interatomic potentials. *Multiscale Model. Sim.* **14**, 1153–1173 (2016).
59. Thompson, A. P., Swiler, L. P., Trott, C. R., Foiles, S. M. & Tucker, G. J. Spectral neighbor analysis method for automated generation of quantum-accurate interatomic potentials. *J. Comput. Phys.* **285**, 316–330 (2015).
60. Körmann, F. & Sluiter, M. H. Interplay between lattice distortions, vibrations and phase stability in NbMoTaW high entropy alloys. *Entropy* **18**, 403 (2016).

61. Fernández-Caballero, A., Wróbel, J. S., Mummery, P. M. & Nguyen-Manh, D. Short-range order in high entropy alloys: theoretical formulation and application to Mo-Nb-Ta-VW system. *J. Phase Equilib. Diff.* **38**, 391–403 (2017).
62. Singh, P., Smirnov, A. V. & Johnson, D. D. Ta-Nb-Mo-W refractory high-entropy alloys: anomalous ordering behavior and its intriguing electronic origin. *Phys. Rev. Mater.* **2**, 055004 (2018).
63. Grabowski, B. et al. Ab initio vibrational free energies including anharmonicity for multicomponent alloys. *npj Comput. Mater.* **5**, 80 (2019).
64. Li, Q.-J., Sheng, H. & Ma, E. Strengthening in multi-principal element alloys with local-chemical-order roughened dislocation pathways. *Nat. Commun.* **10**, 3563 (2019).
65. Yu, P., Du, J.-P., Shinzato, S., Meng, F.-S. & Ogata, S. Theory of history-dependent multi-layer generalized stacking fault energy—a modeling of the micro-substructure evolution kinetics in chemically ordered medium-entropy alloys. *Acta Mater.* **224**, 117504 (2022).
66. Niu, C. et al. Spin-driven ordering of Cr in the equiatomic high entropy alloy NiFeCrCo. *Appl. Phys. Lett.* **106**, 161906 (2015).
67. Mizuno, M., Sugita, K. & Araki, H. Prediction of short-range order in CrMnFeCoNi high-entropy alloy. *Results Phys.* **34**, 105285 (2022).
68. Feng, W., Qi, Y. & Wang, S. Effects of Mn and Al addition on structural and magnetic properties of FeCoNi-based high entropy alloys. *Mater. Res. Express* **5**, 106511 (2018).
69. Singh, P. et al. Tuning phase stability and short-range order through al doping in $(CoCrFeMn)_{100-x}Al_x$ high-entropy alloys. *Phys. Rev. Mater.* **3**, 075002 (2019).
70. Koch, L. et al. Local segregation versus irradiation effects in high-entropy alloys: steady-state conditions in a driven system. *J. Appl. Phys.* **122**, 105106 (2017).
71. Chen, S. et al. Simultaneously enhancing the ultimate strength and ductility of high-entropy alloys via short-range ordering. *Nat. Commun.* **12**, 4953 (2021).
72. El-Atwani, O. et al. Outstanding radiation resistance of tungsten-based high-entropy alloys. *Sci. Adv.* **5**, eaav2002 (2019).
73. Sobieraj, D. et al. Chemical short-range order in derivative Cr-Ta-Ti-V-W high entropy alloys from the first-principles thermodynamic study. *Phys. Chem. Chem. Phys.* **22**, 23929–23951 (2020).
74. Antillon, E., Woodward, C., Rao, S. & Akdim, B. Chemical short range order strengthening in BCC complex concentrated alloys. *Acta Mater.* **215**, 117012 (2021).
75. Huang, X. et al. Atomistic simulation of chemical short-range order in HfNbTaZr high entropy alloy based on a newly-developed interatomic potential. *Mater. Design* **202**, 109560 (2021).
76. Kostiuchenko, T., Ruban, A. V., Neugebauer, J., Shapeev, A. & Körmann, F. Short-range order in face-centered cubic VCoNi alloys. *Phys. Rev. Mater.* **4**, 113802 (2020).
77. Antillon, E., Woodward, C., Rao, S. I., Akdim, B. & Parthasarathy, T. Chemical short range order strengthening in a model FCC high entropy alloy. *Acta Mater.* **190**, 29–42 (2020).
78. Singh, P., Smirnov, A. V., Alam, A. & Johnson, D. D. First-principles prediction of incipient order in arbitrary high-entropy alloys: exemplified in $Ti_{0.25}CrFeNiAl_x$. *Acta Mater.* **189**, 248–254 (2020).
79. Körmann, F., Kostiuchenko, T., Shapeev, A. & Neugebauer, J. B2 ordering in body-centered-cubic AlNbTiV refractory high-entropy alloys. *Phys. Rev. Mater.* **5**, 053803 (2021).
80. Lun, Z. et al. Cation-disordered rocksalt-type high-entropy cathodes for Li-ion batteries. *Nat. Mater.* **20**, 214–221 (2021).
81. Jiang, B. et al. Probing the local site disorder and distortion in pyrochlore high-entropy oxides. *J. Am. Chem. Soc.* **143**, 4193–4204 (2020).
82. Wang, S. et al. Chemical short-range ordering and its strengthening effect in refractory high-entropy alloys. *Phys. Rev. B* **103**, 104107 (2021).
83. Zhang, B., Ding, J. & Ma, E. Chemical short-range order in body-centered-cubic TiZrHfNb high-entropy alloys. *Appl. Phys. Lett.* **119**, 201908 (2021).
84. He, Q. et al. Understanding chemical short-range ordering/demixing coupled with lattice distortion in solid solution high entropy alloys. *Acta Mater.* **216**, 117140 (2021).
85. Pei, Z., Li, R., Gao, M. C. & Stocks, G. M. Statistics of the NiCoCr medium-entropy alloy: novel aspects of an old puzzle. *npj Comput. Mater.* **6**, 122 (2020).
86. Singh, P. & Johnson, D. D. Designing order-disorder transformation in high-entropy ferritic steels. *J. Mater. Res.* **37**, 136–144 (2022).
87. Zhang, Y. H., Zhuang, Y., Hu, A., Kai, J.-J. & Liu, C. T. The origin of negative stacking fault energies and nano-twin formation in face-centered cubic high entropy alloys. *Scripta Mater.* **130**, 96–99 (2017).
88. Ikeda, Y., Körmann, F., Tanaka, I. & Neugebauer, J. Impact of chemical fluctuations on stacking fault energies of CrCoNi and CrMnFeCoNi high entropy alloys from first principles. *Entropy* **20**, 655 (2018).
89. Zhao, S., Osetsky, Y., Stocks, G. M. & Zhang, Y. Local-environment dependence of stacking fault energies in concentrated solid-solution alloys. *npj Comput. Mater.* **5**, 13 (2019).
90. Fukushima, T. et al. Local energies and energy fluctuations—applied to the high entropy alloy CrFeCoNi. *J. Phys. Soc. Jpn* **86**, 114704 (2017).
91. Meshkov, E., Novoselov, I., Shapeev, A. & Yanilkin, A. Sublattice formation in CoCrFeNi high-entropy alloy. *Intermetallics* **112**, 106542 (2019).
92. Jian, W.-R., Wang, L., Bi, W., Xu, S. & Beyerlein, I. J. Role of local chemical fluctuations in the melting of medium entropy alloy CoCrNi. *Appl. Phys. Lett.* **119**, 121904 (2021).
93. Varvenne, C., Luque, A. & Curtin, W. A. Theory of strengthening in fcc high entropy alloys. *Acta Mater.* **118**, 164–176 (2016).
94. Maresca, F. & Curtin, W. A. Mechanistic origin of high strength in refractory BCC high entropy alloys up to 1900 K. *Acta Mater.* **182**, 235–249 (2020).
95. Jian, W.-R. et al. Effects of lattice distortion and chemical short-range order on the mechanisms of deformation in medium entropy alloy CoCrNi. *Acta Mater.* **199**, 352–369 (2020).
96. Yang, X. et al. Chemical short-range order strengthening mechanism in CoCrNi medium-entropy alloy under nanoindentation. *Scripta Mater.* **209**, 114364 (2022).
97. Schön, C. G. On short-range order strengthening and its role in high-entropy alloys. *Scripta Mater.* **196**, 113754 (2021).
98. Yin, S. et al. Atomistic simulations of dislocation mobility in refractory high-entropy alloys and the effect of chemical short-range order. *Nat. Commun.* **12**, 4873 (2021).
99. Li, X.-G., Chen, C., Zheng, H., Zuo, Y. & Ong, S. P. Complex strengthening mechanisms in the NbMoTaW multi-principal element alloy. *npj Comput. Mater.* **6**, 70 (2020).
100. Kristoffersen, H. & Rossmeisl, J. Local order in AgAuCuPdPt high-entropy alloy surfaces. *J. Phys. Chem. C* **126**, 6782–6790 (2022).
101. Wynblatt, P. & Chatain, D. Modeling grain boundary and surface segregation in multicomponent high-entropy alloys. *Phys. Rev. Mater.* **3**, 054004 (2019).
102. Chatain, D. & Wynblatt, P. Surface segregation in multicomponent high entropy alloys: atomistic simulations versus a multilayer analytical model. *Comput. Mater. Sci.* **187**, 110101 (2021).

103. Ferrari, A. & Körmann, F. Surface segregation in Cr-Mn-Fe-Co-Ni high entropy alloys. *Appl. Surf. Sci.* **533**, 147471 (2020).
104. Podryabinkin, E. V. & Shapeev, A. V. Active learning of linearly parametrized interatomic potentials. *Comput. Mater. Sci.* **140**, 171–180 (2017).
105. Novikov, I., Grabowski, B., Körmann, F. & Shapeev, A. Magnetic moment tensor potentials for collinear spin-polarized materials reproduce different magnetic states of bcc Fe. *npj Comput. Mater.* **8**, 13 (2022).

Acknowledgements

A.F. and F.K. acknowledge funding from Nederlandse Organisatie voor Wetenschappelijk Onderzoek (NWO)/Stichting voor de Technische Wetenschappen (STW), VIDI grant no. 15707. M.A. acknowledges funding from the US Department of Energy, Office of Science, Office of Basic Energy Sciences, Materials Sciences and Engineering Division, under contract no. DE-AC02-05-CH11231 within the Damage-Tolerance in Structural Materials (KC 13) program. F.K. acknowledges funding by the Deutsche Forschungsgemeinschaft (German Research Foundation) through project no. 429582718 and J.N. through projects nos. 405621160 and 405621217.

Author contributions

A.F. wrote the manuscript with comments and input from F.K., M.A. and J.N. All authors contributed to discussions and commented on the manuscript.

Competing interests

The authors declare no competing interests.

Additional information

Correspondence should be addressed to Fritz Körmann or Jörg Neugebauer.

Peer review information *Nature Computational Science* thanks Maryam Ghazisaeidi and the other, anonymous, reviewer(s) for their contribution to the peer review of this work. Primary Handling Editor: Jie Pan, in collaboration with the *Nature Computational Science* team.